



Published in final edited form as:

Ann Surg Oncol. 2017 July ; 24(7): 1897–1903. doi:10.1245/s10434-017-5804-8.

Optical see-through cancer vision goggles enable direct patient visualization and real-time fluorescence-guided oncologic surgery

Suman B. Mondal, PhD^{1,2}, Shengkui Gao, PhD³, Nan Zhu, PhD⁴, LeMoyne Hebimana-Griffin, BS^{1,2}, Walter J. Akers, PhD, DVM¹, Rongguang Liang, PhD⁴, Viktor Gruev, PhD³, Julie Margenthaler, MD⁵, and Samuel Achilefu, PhD^{1,2,6}

¹Department of Radiology, Washington University School of Medicine, St Louis, MO

²Department of Biomedical Engineering, Washington University in St Louis, St Louis, MO

³Department of Computer Science and Engineering, Washington University in St Louis, St Louis, MO

⁴College of Optical Science, The University of Arizona

⁵Department of Surgery, Washington University School of Medicine, St Louis, MO

⁶Department of Biochemistry and Molecular Biophysics, Washington University School of Medicine, St Louis, MO

Abstract

Background—The inability to directly visualize the patient and surgical site limits the use of current near infrared fluorescence-guided surgery systems for real-time sentinel lymph node biopsy and tumor margin assessment.

Methods—We evaluated an optical see-through goggle augmented imaging and navigation system (GAINS) for near-infrared fluorescence-guided surgery. Tumor-bearing mice injected with a near infrared cancer-targeting agent underwent fluorescence-guided tumor resection. Female Yorkshire pigs received hind leg intradermal indocyanine green injection and underwent fluorescence-guided popliteal lymph node resection. Four breast cancer patients received ^{99m}Tc-sulfur colloid and indocyanine green retroareolarly, before undergoing sentinel lymph node biopsy using radioactive tracking and fluorescence imaging. Three other breast cancer patients received indocyanine green retroareolarly before undergoing standard-of-care partial mastectomy, followed by fluorescence imaging of resected tumor and tumor cavity for margin assessment.

Results—Using near-infrared fluorescence from the dyes, the optical see-through GAINS accurately identified all mouse tumors, pig lymphatics, and 4 pig popliteal lymph nodes with high signal-to-background ratio. In 4 human breast cancer patients, 11 sentinel lymph nodes were identified with a detection sensitivity of 86.67± 0.27% for radioactive tracking and 100% for

Corresponding Authors: Samuel Achilefu, PhD; address – Mallinckrodt Institute of Radiology, Washington University School of Medicine, 4515 McKinley Ave, St Louis, MO 63110; achilefu@wustl.edu; telephone - 314.362.8599; fax - 314.747.5191.

Disclosure: The authors declare no commercial interest in the reported research.

GAINS. Tumor margin status was accurately predicted by GAINS in all three patients, including clear margins in patients 1 and 2 and positive margins in patient 3 as confirmed by paraffin embedded section histopathology.

Conclusions—The optical see-through GAINS prototype enhances near infrared fluorescence-guided surgery for sentinel lymph node biopsy and tumor margin assessment in breast cancer patients without disrupting the surgical workflow in the operating room.

Breast cancer is the most common cancer and the leading cause of cancer death in women in the US¹, with breast-conserving surgery (BCS) as the standard-of-care for early stage breast cancer. BCS is usually accompanied by sentinel lymph node (SLN) biopsy² for disease staging³, using radioactive and blue dye tracking^{4–7}. However, radioactive tracers expose patients and caregivers to ionizing radiation and require the involvement of nuclear medicine trained personnel, increasing costs and difficulty in scheduling surgery. Additionally, the strict regulatory hurdles prevent the use of radioisotopes in some surgical centers. Although blue dyes can overcome some of these limitations, tissue autofluorescence and shallow penetration of visible light in tissue preclude visualizing deep-seated lymph nodes⁸. These dyes also pose the risk of anaphylactic reactions in 1–3% of patients⁹. Perhaps a greater challenge in BCS is positive margin resection¹⁰. Approximately 25% of women undergoing BCS have positive surgical margins that can lead to a two-fold increase in ipsilateral tumor recurrence¹¹. As a result, the presence of positive margins requires repeat operation. Currently, significant variability exists in patient outcomes based on the facility where the surgery is performed, surgeon experience, and patient's age and tumor characteristics^{12–14}.

Near-infrared (NIR) fluorescence-guided surgery (FGS) has been shown to facilitate intraoperative SLN biopsy^{15–23} and tumor margin assessment²⁴. Several intraoperative NIR-FGS systems have been developed and tested clinically^{21,24–29}. However, they often suffer from a large hardware footprint in an already crowded operating room. Typically, the camera's and surgeon's field of view do not match, which necessitates a learning curve for system usage. Current FGS systems display the information on remote monitors that require the surgeon to look away from the surgical bed. Additionally, using handheld devices require the surgeon to stop working or need someone from the surgical team to operate the instrument. The combination of these factors can disrupt standard surgical workflow and may increase surgery time.

We previously developed a goggle augmented imaging and navigation system (GAINS)⁸ for real-time NIR FGS that allowed accurate tumor resection in mouse models of cancer and enabled SLN visualization in human breast cancer and melanoma patients with high sensitivity. GAINS detects both anatomic color reflectance and NIR fluorescence from contrast agents, displaying accurately aligned superimposed color-NIR images via a head-mounted display (HMD) worn by the surgeon⁸. This system displayed the images in a video-see-through mode, which obstructed direct visualization of the patient. Reliance on a video feed for open surgery minimizes natural visual and tactile skills that surgeons utilize routinely during surgery. Based on the feedback from surgeons, we have developed an optical see-through (OST) HMD system that allows direct visualization of the surgical bed with provision to project fluorescence information directly to the user's eyes³⁰. In this study,

we performed in vivo evaluation of the OST GAINS prototype in a subcutaneous mouse model of cancer for guiding tumor resection, lymphatic tracking and LN resection in a porcine model. We also evaluated the system for SLN biopsy and tumor margin assessment in human breast cancer patients.

METHODS

Fluorescence-guided surgery

Real-time intraoperative FGS was performed using the OST GAINS prototype (Fig. 1) which was described in detail earlier³⁰. Briefly, the GAINS uses a focus-adjustable camera to capture color reflectance and NIR fluorescence and generates accurately aligned color-NIR superimposed images. These images are displayed via a custom OST HMD that allows direct visual access to the surgical field, with contrast- and transparency-adjusted projection of fluorescence information. A 780 nm, 0.8 W laser (B&W Tek, Newark, DE) provides the NIR illumination. White light illumination is provided by standard surgical light (Sup Fig. 1), covered with a short-pass film filter³¹ to minimize the NIR bleed through into the fluorescence detection channel of the GAINS camera. System evaluation is described in the Supplementary Methods.

Animal studies

All animal studies were approved by the Washington University Animal Studies Committee. Three 6 week-old Balb/c nu/nu mice were subcutaneously injected with 10⁶ prostate neuroendocrine cancer cells (PNEC30, ATCC, Manassas, VA) cells in their left hind flanks. They were injected with a tumor-targeted NIR contrast agent LS301⁸ (0.441 mg/kg) via tail vein injection, 10–12 days after tumor implantation. At 24 h post-injection, the mice were anesthetized using 2% isoflurane and OST GAINS was used for fluorescence-guided tumor resection. All resected tissues were preserved for frozen section histopathologic analysis.

Three 35-kg female Yorkshire pigs received 0.04 mg/kg atropine and 0.45 mg/kg Telazol, ketamine, and xylazine intramuscularly. Anesthesia was subsequently maintained with isoflurane (1–5% v/v in O₂) by intubation. ICG (0.043 mg/kg, Sigma-Aldrich, St. Louis, MO) was injected intradermally into the hind leg. OST GAINS was used to non-invasively track lymphatic ICG circulation, to locate, guide incision and resection of popliteal LNs. Resected LNs were preserved in formalin. All pigs were euthanized by intravenous potassium chloride.

Histology

Fresh-frozen tissue samples were cryo-sectioned to create 10 μm tissue sections which were imaged for NIR fluorescence, followed by hematoxylin and eosin staining. The same areas were then imaged under brightfield for co-registration with NIR fluorescence using an epifluorescence microscope (BX51 Olympus, Center Valley, PA).

Human pilot study

The human pilot study was approved by the Institutional Review Board at Washington University and registered on the clinicaltrials.gov website (NCT02316795). Women, with

newly diagnosed clinically node-negative breast cancer, negative nodal basin clinical exam and scheduled to undergo partial mastectomy with SLN biopsy were enrolled for the study. All patients gave informed consent for this HIPAA-compliant study and data was deidentified.

All patients (n=7) received a single deposit subcutaneous injection of ^{99m}Tc -sulfur colloid (834 μCi , 1 ml) 2–3 h before surgery. Patients were injected with ICG (25 mg, 5 ml) in the retroareolar breast, peritumorally using 4 deposits around the primary tumor area, followed by site massage for 5 min. About 10–15 min after injection, the surgeon performed standard-of-care SLN biopsy or partial mastectomy. The methods for patients undergoing sentinel lymph node biopsy (n=4) and those undergoing intraoperative tumor margin assessment (n=3) are described in the Supplementary Methods. The use of both ICG staining and radioactivity enhanced the selective identification of SLNs. Tumor margins were evaluated by specimen radiography³² before the tumor tissue were preserved for histopathologic evaluation. All OST GAINS components were sterilized by thoroughly wiping the system with sterile, 70% alcohol wipes before entering the operating room for each procedure (see Supplementary Methods for additional information).

Statistical analysis

Statistical analysis was performed using OriginPro8 (OriginLab Corp., Northampton, MA). Signal-to-background ratios (SBRs), and sensitivity were expressed as mean and standard deviations. Paired t-tests were used to compare fluorescence signal for non-invasive and invasive imaging in the mouse model of tumor, fluorescence signal during transcutaneous lymphatic tracking and exposed lymph nodes in pigs and sensitivity of SLN detection by OST GAINS and radioactive tracking. $P < 0.05$ were considered statistically significant.

RESULTS

Tumor resection in mice

The OST GAINS allowed direct visual access to the surgical bed while projecting real-time high-contrast fluorescence information to guide complete tumor resection in three mice (Fig. 1). Transcutaneous tumor fluorescence was detected with an SBR of 1.45 ± 0.24 and guided incision to expose the tumors. Fluorescence from exposed tumors was detected with an SBR of 1.49 ± 0.13 and guided tumor resection. Both tumor and background fluorescence detected after skin deflection was significantly higher than that observed with intact skin ($P < 0.05$ and $P < 0.01$), signifying the more reflective nature of the peritoneum. There was no statistically significant difference between the SBR for transcutaneous and exposed tumor fluorescence ($P = 0.37$) (Sup. Table 1). Survey of the tumor bed for residual fluorescence showed that no suspected tumor tissue was left behind. All tissue were confirmed to be cancerous by histopathology.

Lymphatic tracking in pigs

OST GAINS detected transcutaneous lymphatic fluorescence in three pigs (Fig 1) with an SBR of 2.74 ± 1.74 . Fluorescence lymphatic tracking from injection site successfully guided incision and resection of all popliteal LNs (**Vid. 1**) without using radioactive tracking. A

total of 4 popliteal LNs were detected with an SBR of 3.19 ± 1.81 that allowed their accurate resection. Fluorescence from exposed LN as well as background tissue was significantly higher than fluorescence from transcutaneous lymphatics and intact skin ($P < 0.01$) (Sup. Table 1). The LN SBR was significantly higher than the SBR for transcutaneous lymphatics ($P < 0.05$), suggesting that pig peritoneum is less reflective than mouse peritoneum, during NIR imaging.

SLN biopsy in human breast cancer patients

Before human use, a surgeon evaluated the OST HMD system in a pre-clinical operating room using ICG phantom (see Supplementary Results). The patient characteristics are listed in Table 1. The direct visual access to the surgical field allowed the surgeon to make tissue incision and resection while wearing the OST GAINS prototype (Fig 2). The fluorescence projection to the HMD was turned on when requested by the surgeon for SLN visualization, and its contrast was remotely controlled, based on surgeon feedback and ambient light to ensure visibility of fluorescence as well as underlying tissue (Sup Fig 2). All fluorescence guidance was performed without turning off the surgical lights. No adverse reactions associated with the use of ICG or the OST GAINS prototype occurred and no postoperative complications were observed. A total of 11 SLNs were identified from 4 patients with a mean of 2.2 ± 0.98 SLNs identified per patient (Table 1). The OST GAINS identified 11 (100%) SLNs with a detection sensitivity of 100% and SBR of 2.14 ± 0.83 (Table 1). Radioactive tracking identified 9 (81.82%) SLNs with a detection sensitivity of $86.67 \pm 0.27\%$. However, there was no statistically significant difference between the detection sensitivities of the fluorescence and radioactive methods ($P = 0.374$) (Table 1). This was because radioactive tracking did not identify two SLNs in one of the patients, while accurately identifying all SLNs in rest of the patients. Due to this skewed distribution and the small number of patients, we do not see a statistically significant difference between the detection sensitivities of the two methods.

Tumor margin assessment in human breast cancer patients

The OST GAINS enabled real-time visualization of ICG fluorescence in the tumor tissue (Vid 2) and tumor cavity (Vid 3). The patient and tumor characteristics are listed in Table 2. The fluorescence information was projected when requested by the surgeon for visualizing the resected tumor tissue and the cavity. No adverse reactions associated with the use of ICG or the OST GAINS prototype occurred and no postoperative complications were observed. OST GAINS accurately predicted margin status in all three patients and performed better than gross visual inspection and specimen radiography (Table 2). Minimal or no fluorescence was observed in the resected tissue or the tumor cavity in patients 1 and 2, and clear margins were predicted based on ICG fluorescence. In patient 3, high fluorescence area was observed on the lumpectomy sample and the edges of the cavity (Fig. 3), leading to a prediction of positive margins. All margin predictions were confirmed by the final pathology report.

DISCUSSION

Our study demonstrates that the OST GAINS facilitates the integration of FGS in the surgical workflow. The see-through feature allows direct visualization of the surgical field with the provision of fluorescence information whenever needed. Controllable contrast and opacity of projection allowed optimization of tissue and tumor visualization. Display options for the surgeon include the projection of pseudo-colored fluorescence or superimposed pseudo-colored fluorescence-color images (Sup. Fig. 3). Our system mirrors the surgeon's view on a remote laptop, and a custom graphical user interface allows real-time modifications of the imaging parameters by a member of the surgical team⁸. This feature enables users to implement the surgeon feedback without disrupting the ongoing surgery. Camera focus was adjusted to compensate for large head movements and to ensure the image was always in focus. Additionally, the built-in fail-safe of the see-through feature can allow surgeons to continue routine surgery in case of system failure to project fluorescence information. All operations were performed under regular OR surgical lights, allowing real-time FGS with minimal disruptions.

The OST GAINS was able to guide complete tumor resection in mice. In pigs, the imaging system allowed non-invasive transcutaneous lymphatic tracking and the identification of LNs using fluorescence guidance only. Recent studies have reported the feasibility of using optical imaging for SLN biopsy and tumor margin assessment^{24,33,34}. Our results demonstrate the feasibility of detecting SLNs using FGS with identical sensitivity as the standard radioactive tracking method. Using ICG and FGS, we also demonstrate real-time assessment of tumor margins with better accuracy than specimen radiography. The intraoperative margin prediction based on ICG fluorescence was correlated post-operatively with pathology. ICG does not possess tumor specificity via an active cancer-targeting mechanism. However, previous studies have shown the feasibility of using ICG fluorescence to detect human tumors in the operating room^{24,35}. ICG can passively accumulate in tumors because of the distorted vasculature and poor lymphatics. Peritumoral injection of ICG, followed by breast massage for a few minutes before imaging in about 15 minutes post injection allows the dye to transiently perfuse the periphery of tumors. In addition to enhanced permeation and retention effect, the binding of ICG to blood proteins such as albumin in the tumor environment caused by leaky vasculature is also known to facilitate its uptake in tumors. We attribute the detection of positive margins to a combination of factors that includes positive pressure during breast massage, which aids in the distribution and drainage of ICG, poor lymphatics around the tumor, rapid albumin binding, and sufficient time for selective retention of ICG in the tumor environment before cancer resection. The fluorescence data were not used for medical decision. Instead, the projected fluorescence provided additional information for the surgeon to assess the surgical margins intraoperatively. Although a large patient population is needed to validate the findings of this feasibility study, the encouraging results provide a firm basis to pursue this line of research.

Through its unique wearable design and direct visual access to the surgical field, the OST GAINS overcomes some of the limitations of current standalone and handheld NIR FGS systems. However, comparative evaluation of the OST GAINS prototype and other fluorescence imaging technologies is needed to delineate the strengths of each FGS system

for a particular clinical application. The OST GAINS has some limitations. It currently performs final image processing on a laptop, tethering the surgeon to a cart carrying the laptop via a wired connection. Additionally, a mismatch in the perceived distance of the projected fluorescence and actual object distance seen by the surgeon may cause parallax. Efforts are currently underway to ensure complete onboard image processing, with wireless data transmission, as well as to ensure minimal parallax by adjustment of perceived distance of projected fluorescence images.

CONCLUSION

The OST GAINS prototype enabled FGS with direct visual access to the surgical field under ambient light. We demonstrated the feasibility of accurate real-time intraoperative SLN biopsy and tumor margin assessment in breast cancer patients without disrupting the surgical workflow.

Supplementary Material

Refer to Web version on PubMed Central for supplementary material.

Acknowledgments

APPENDIXES

Funding for this project was supported primarily by funds from the US National Institutes of Health (NIH) NCI (R01 CA171651) and in part by NCI grants U54 CA199092, P50 CA094056 and P30 CA091842; NIBIB (R01 EB021048, R01 EB007276 and R01 EB008111); and shared instrumentation grants (S10 OD016237 and S10 RR031625). SBM was supported in part by the Foundation for Barnes-Jewish Hospital and the Children's Discovery Institute at St. Louis Children's Hospital. LHB was supported in part by NCI grant U54CA199092S1. We thank Dr. Michael Talcott for assistance the porcine study.

References

1. Siegel RL, Miller KD, Jemal A. Cancer statistics, 2015. *CA Cancer J Clin*. 2015; 65(1):5–29. [PubMed: 25559415]
2. Giuliano AE, Kirgan DM, Guenther JM, Morton DL. Lymphatic mapping and sentinel lymphadenectomy for breast cancer. *Ann Surg*. 1994; 220(3):391–98. [PubMed: 8092905]
3. Cox CE, Pendas S, Cox JM, et al. Guidelines for sentinel node biopsy and lymphatic mapping of patients with breast cancer. *Ann Surg*. 1998; 227(5):645–51. [PubMed: 9605656]
4. Goyal A, Newcombe RG, Chhabra A, Mansel RE, Group AT. Factors affecting failed localisation and false-negative rates of sentinel node biopsy in breast cancer—results of the ALMANAC validation phase. *Breast Cancer Res Treat*. 2006; 99(2):203–08. [PubMed: 16541308]
5. Krag DN, Anderson SJ, Julian TB, et al. Technical outcomes of sentinel-lymph-node resection and conventional axillary-lymph-node dissection in patients with clinically node-negative breast cancer: results from the NSABP B-32 randomised phase III trial. *Lancet Oncol*. 2007; 8(10):881–88. [PubMed: 17851130]
6. Straver ME, Meijnen P, van Tienhoven G, et al. Sentinel node identification rate and nodal involvement in the EORTC 10981–22023 AMAROS trial. *Ann Surg Oncol*. 2010; 17(7):1854–61. [PubMed: 20300966]
7. Zavagno G, De Salvo GL, Scalco G, et al. A Randomized clinical trial on sentinel lymph node biopsy versus axillary lymph node dissection in breast cancer: results of the Sentinella/GIVOM trial. *Ann Surg*. 2008; 247(2):207–13. [PubMed: 18216523]

8. Mondal SB, Gao S, Zhu N, et al. Binocular Goggle Augmented Imaging and Navigation System provides real-time fluorescence image guidance for tumor resection and sentinel lymph node mapping. *Sci Rep*. 2015; 5:12117. [PubMed: 26179014]
9. Bézu C, Coutant C, Salengro A, Daraï E, Rouzier R, Uzan S. Anaphylactic response to blue dye during sentinel lymph node biopsy. *Surg Oncol*. 2011; 20(1):e55–e59. [PubMed: 21074413]
10. Singletary SE. Surgical margins in patients with early-stage breast cancer treated with breast conservation therapy. *Am J Surg*. 2002; 184(5):383–93. [PubMed: 12433599]
11. Moran MS, Schnitt SJ, Giuliano AE, et al. Society of Surgical Oncology–American Society for Radiation Oncology consensus guideline on margins for breast-conserving surgery with whole-breast irradiation in stages I and II invasive breast cancer. *Ann Surg Oncol*. 2014; 21(3):704–16. [PubMed: 24515565]
12. McCahill LE, Single RM, Aiello Bowles EJ, et al. Variability in reexcision following breast conservation surgery. *JAMA*. 2012; 307(5):467–75. [PubMed: 22298678]
13. Morrow M, Jagsi R, Alderman AK, et al. Surgeon recommendations and receipt of mastectomy for treatment of breast cancer. *JAMA*. 2009; 302(14):1551–56. [PubMed: 19826024]
14. Mullen R, Macaskill EJ, Khalil A, et al. Involved anterior margins after breast conserving surgery: Is re-excision required? *Eur J Surg Oncol*. 2012; 38(4):302–06. [PubMed: 22285907]
15. Hirche C, Murawa D, Mohr Z, Kneif S, Hunerbein M. ICG fluorescence-guided sentinel node biopsy for axillary nodal staging in breast cancer. *Breast Cancer Res Treat*. 2010; 121(2):373–78. [PubMed: 20140704]
16. Hojo T, Nagao T, Kikuyama M, Akashi S, Kinoshita T. Evaluation of sentinel node biopsy by combined fluorescent and dye method and lymph flow for breast cancer. *Breast*. 2010; 19(3):210–13. [PubMed: 20153649]
17. Kitai T, Inomoto T, Miwa M, Shikayama T. Fluorescence navigation with indocyanine green for detecting sentinel lymph nodes in breast cancer. *Breast Cancer*. 2005; 12(3):211–15. [PubMed: 16110291]
18. Murawa D, Hirche C, Dresel S, Hunerbein M. Sentinel lymph node biopsy in breast cancer guided by indocyanine green fluorescence. *Br J Surg*. 2009; 96(11):1289–94. [PubMed: 19847873]
19. Sevick-Muraca EM, Sharma R, Rasmussen JC, et al. Imaging of lymph flow in breast cancer patients after microdose administration of a near-infrared fluorophore: feasibility study. *Radiology*. 2008; 246(3):734–41. [PubMed: 18223125]
20. Tagaya N, Yamazaki R, Nakagawa A, et al. Intraoperative identification of sentinel lymph nodes by near-infrared fluorescence imaging in patients with breast cancer. *Am J Surg*. 2008; 195(6):850–53. [PubMed: 18353274]
21. Troyan SL, Kianzad V, Gibbs-Strauss SL, et al. The FLARE intraoperative near-infrared fluorescence imaging system: a first-in-human clinical trial in breast cancer sentinel lymph node mapping. *Ann Surg Oncol*. 2009; 16(10):2943–52. [PubMed: 19582506]
22. Mieog JS, Troyan SL, Hutteman M, et al. Toward optimization of imaging system and lymphatic tracer for near-infrared fluorescent sentinel lymph node mapping in breast cancer. *Ann Surg Oncol*. 2011; 18(9):2483–91. [PubMed: 21360250]
23. van der Vorst JR, Schaafsma BE, Verbeek FP, et al. Randomized comparison of near-infrared fluorescence imaging using indocyanine green and 99(m) technetium with or without patent blue for the sentinel lymph node procedure in breast cancer patients. *Ann Surg Oncol*. 2012; 19(13):4104–11. [PubMed: 22752379]
24. Keating J, Tchou J, Okusanya O, et al. Identification of breast cancer margins using intraoperative near-infrared imaging. *J Surg Oncol*. 2016; 113(5):508–14. [PubMed: 26843131]
25. Hirche C, Engel H, Kolios L, et al. An experimental study to evaluate the Fluobeam 800 imaging system for fluorescence-guided lymphatic imaging and sentinel node biopsy. *Surg Innov*. 2013; 20(5):516–23. [PubMed: 23275469]
26. Tobis S, Knopf JK, Silvers CR, et al. Near infrared fluorescence imaging after intravenous indocyanine green: initial clinical experience with open partial nephrectomy for renal cortical tumors. *Urology*. 2012; 79(4):958–64. [PubMed: 22336035]

27. Gotoh K, Yamada T, Ishikawa O, et al. A novel image-guided surgery of hepatocellular carcinoma by indocyanine green fluorescence imaging navigation. *J Surg Oncol.* 2009; 100(1):75–79. [PubMed: 19301311]
28. Mondal SB, Gao S, Zhu N, Liang R, Gruev V, Achilefu S. Real-time Fluorescence Image-Guided Oncologic Surgery. *Adv Cancer Res.* 2014; 124:171–211. [PubMed: 25287689]
29. van den Berg NS, Miwa M, KleinJan GH, et al. (Near-Infrared) Fluorescence-Guided Surgery Under Ambient Light Conditions: A Next Step to Embedment of the Technology in Clinical Routine. *Ann Surg Oncol.* 2016; 23:2586–95. [PubMed: 27020586]
30. Zhu N, Huang CY, Mondal S, et al. Compact wearable dual-mode imaging system for real-time fluorescence image-guided surgery. *J Biomed Opt.* 2015; 20(9):96010.
31. Zhu N, Mondal S, Gao S, Achilefu S, Gruev V, Liang R. Engineering light-emitting diode surgical light for near-infrared fluorescence image-guided surgical systems. *J Biomed Opt.* 2014; 19(7):076018. [PubMed: 25057962]
32. Rua C, Lebas P, Michenet P, Ouldamer L. Evaluation of lumpectomy surgical specimen radiographs in subclinical, in situ and invasive breast cancer, and factors predicting positive margins. *Diagnostic and Interventional Imaging.* 2012; 93(11):871–77. [PubMed: 23021868]
33. Judy RP, Keating JJ, DeJesus EM, et al. Quantification of tumor fluorescence during intraoperative optical cancer imaging. *Sci Rep.* 2015; 5:16208. [PubMed: 26563091]
34. Zysk AM, Chen K, Gabrielson E, et al. Intraoperative Assessment of Final Margins with a Handheld Optical Imaging Probe During Breast-Conserving Surgery May Reduce the Reoperation Rate: Results of a Multicenter Study. *Ann Surg Oncol.* 2015; 22(10):3356–62. [PubMed: 26202553]
35. Liu Y, Zhao YM, Akers W, et al. First in-human intraoperative imaging of HCC using the fluorescence goggle system and transarterial delivery of near-infrared fluorescent imaging agent: a pilot study. *Transl Res.* 2013; 162(5):324–31. [PubMed: 23747795]

SYNOPSIS

An optical see-through goggle system enabled real-time fluorescence-guided surgery with direct visual access to the surgical bed. It allowed mouse tumor resection, pig lymph node excision, and sentinel lymph node biopsy as well as tumor margin assessment in breast cancer patients.

Author Manuscript

Author Manuscript

Author Manuscript

Author Manuscript

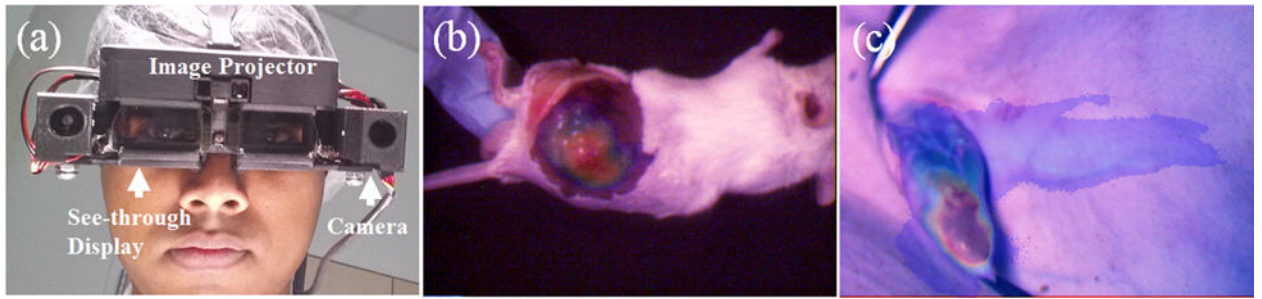


Figure 1. Imaging system and preclinical validation. **a** OST GAINS prototype head-mounted display. **b** Image-guided tumor resection in a mouse model of cancer **c** Lymphatic tracking and LN detection in Yorkshire pigs.

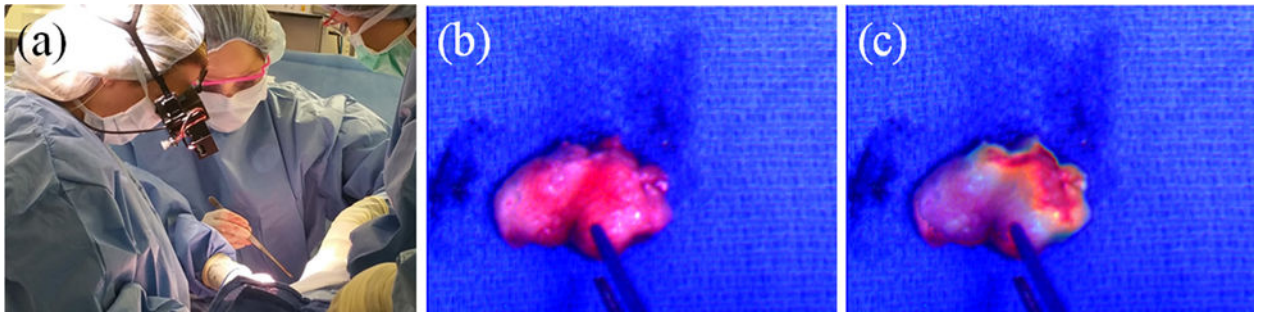


Figure 2. Fluorescence-guided SLN biopsy. **a** The surgeon wearing the GAINS during SLN visualization in a breast cancer patient. **b** The color image of the excised SLN. **c** The superimposed color-fluorescence image of the excised SLN as seen by the surgeon.

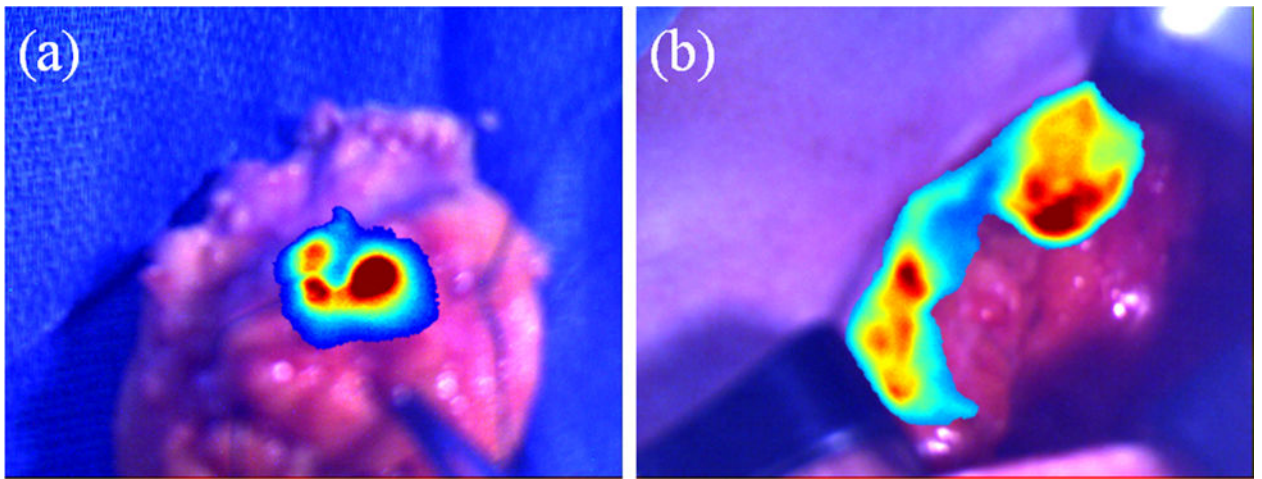


Figure 3. Fluorescence-guided tumor margin assessment. **a.** Lumpectomy sample from patient 3 showing high fluorescence signal. **b.** Lumpectomy cavity from patient 3 showing high fluorescence signal at the edges.

Table 1

Patient characteristics and results for SLN biopsy

No. of patients	4
Age media (range)	63.5 (39–76)
BMI mean (range)	35.5 (26–47)
Diagnosis	
Left Breast Cancer	2 (50%)
Right Breast Cancer	1 (25%)
Bilateral Breast Cancer	1 (25%)
Total no of sentinel lymph node biopsies	5
Procedure	
Left sentinel lymph node biopsy with radioactive tracking and ICG fluorescence	2 (50%)
Right sentinel lymph node biopsy with radioactive tracking and ICG fluorescence	1 (25%)
Bilateral sentinel lymph node biopsy with radioactive tracking and ICG fluorescence	1 (25%)
Injection site ICG	
Retroareolar	5 (100%)
SLNs identified	
Total	11
Mean \pm SD	2.2 \pm 0.98
Method of detection	
Radioactive tracking	9 (81.82%)
ICG-OST GAINS	11 (100%)
Detection sensitivity	
Radioactive tracking, mean \pm SD	86.67 % \pm 0.27
ICG-OST GAINS, mean \pm SD	100% \pm 0.0
Statistical difference	P = 0.374
SBR for fluorescence detection, mean \pm SD	2.14 \pm 0.83
Histology of SLN	
Negative	10 (90.91%)
Macrometastases	1 (9.09%)

Table 2

Patient characteristics and results for tumor margin assessment

No. of patients	3
Age median (range)	52 (41–74)
BMI mean (range)	29.75 (26.57 – 31.8)
Patient 1	
Diagnosis	Right breast cancer
Procedure	Right breast re-excision
Tumor margin assessment	
Gross visual assessment	Negative margins
Specimen radiography	Not performed
ICG-GAINS	Negative margins
Pathology	Negative margins
Patient 2	
Diagnosis	Left breast cancer
Procedure	Left breast partial mastectomy
Tumor margin assessment	
Gross visual assessment	Negative margins
Specimen radiography	Tumor centrally located within specimen
ICG-GAINS	Negative margins
Pathology	Negative margins
Patient 3	
Diagnosis	Left breast cancer
Procedure	Left breast partial mastectomy
Tumor margin assessment	
Gross visual assessment	Negative margins
Specimen radiography	Tumor centrally located within specimen
ICG-GAINS	Positive margins
Pathology	Positive margins